Reconstitution of Bovine A_1 Adenosine Receptors and G Proteins in Phospholipid Vesicles: $\beta\gamma$-Subunit Composition Influences Guanine Nucleotide Exchange and Agonist Binding†

Robert A. Figler,‡ Margaret A. Lindorfer,§ Stephen G. Graber,⊥ James C. Garrison,§ and Joel Linden*,†,||

Departments of Molecular Physiology & Biological Physics, Pharmacology, and Medicine, University of Virginia Health Sciences Center, Charlottesville, Virginia 22908, and Department of Pharmacology and Toxicology, Health Sciences Center, West Virginia University, Morgantown, West Virginia 26506

Received August 12, 1997⊗

ABSTRACT: We have studied the interactions of purified A_1 adenosine receptors and G proteins reconstituted into phospholipid vesicles to investigate how the $\beta\gamma$ composition of G protein heterotrimers influences coupling. Recombinant hexahistidine-tagged bovine A_1 adenosine receptors were expressed in Sf9 cells and purified to homogeneity by sequential chromatography over heparin−sepharose, xanthine amino congener−agarose, and nickel−nitrilotriacetic acid columns. These receptors were reconstituted with pure recombinant G proteins of defined subunit composition. Receptor−G protein complexes containing α_{i2} and $\beta_1\gamma_2$ or $\beta_1\gamma_3$ and stimulated with the agonist, (*R*)-phenylisopropyladenosine, exchange guanine nucleotide 2−3 times more rapidly than do complexes containing $\beta_1\gamma_1$. This difference is not overcome by increasing the concentration of $\beta\gamma$ subunits. Receptor−G protein complexes containing $\beta_1\gamma_1$ also bind less of the agonist, [^{125}I]-iodoaminobenzyladenosine (^{125}I-ABA), than do complexes containing $\beta_1\gamma_3$. Kinetic experiments show that ^{125}I-ABA dissociates 2-fold more rapidly from receptor−G protein complexes containing $\beta_1\gamma_1$ than from complexes containing the other $\beta\gamma$ subunits. The affinity of the interaction between immobilized $G_{\alpha i2}$ subunits and $\beta_1\gamma_1$ or $\beta_1\gamma_2$ measured with an optical biosensor in the absence of receptor is similar. Taken together, these data implicate the γ-subunit in influencing the interaction between the A_1 adenosine receptor and G proteins.

Guanine nucleotide binding proteins (G proteins) are responsible for transducing signals between cell surface receptors and intracellular effectors.[1] There are large numbers of G protein α, β, and γ subunit isoforms, G protein-coupled receptors, and effectors, indicating that a very large number of potential signal transduction pathways are possible (*4*−*7*). However, seven transmembrane domain receptors selectively activate discrete G proteins and effectors in intact cells, raising the question of how specificity in cell signaling is achieved (*5*−*9*).

Typically, investigations have addressed the question of how coupling specificity is achieved by taking one of three basic approaches. Immunological methods including immunoprecipitation of receptor−G protein complexes (*10, 11*) or antibody inhibition of receptor−G protein coupling (*12*−*14*) have been used to identify receptor−G protein interactions. These approaches are limited by the specificity and efficacy of antisera and by the stability of detergent-solubilized receptor−G protein complexes. Antisense suppression (*15*−*20*) or overexpression (*21, 22*) of individual G protein subunits have been used to identify the component parts of particular signaling systems. Conclusions derived from these experiments are limited by the complexity and variability of signaling in intact cells. Finally, the reconstitution of purified receptors and G proteins in cell membranes or phospholipid vesicles has proven to be a powerful technique for investigating receptor−G protein interactions (*1, 23*−*29*). Although this approach is limited by the fact that all of the factors that control the specificity of receptor−G protein coupling in intact cells are not present in reconstituted systems (*6*), the method is advantageous for evaluating the specificity of protein−protein interactions.

Most reconstitution studies have been designed to examine the interaction of a particular receptor with G protein α subunits, and the potential influence of the $\beta\gamma$ subunits on the function of receptor−G protein complexes has not been throughly examined. However, there is mounting evidence that the α subunit is not the sole determinant of coupling and that the $\beta\gamma$ dimer also plays an important role (*1, 29*−*34*). To study the role of the $\beta\gamma$ dimer in the regulation of receptor coupling, we previously utilized the strategy of overexpressing A_1 adenosine receptors in Sf9 cells and reconstituting purified G proteins of defined subunit composition into membrane preparations (*1*). This approach

† Supported by National Institutes of Health Grant Nos. R01-HL37942 (J.L.), DK-19952 (J.C.G.) and American Cancer Society Grant No. IRG-149L (M.A.L.).

‡ Department of Molecular Physiology & Biological Physics.
§ Department of Pharmacology.
|| Department of Medicine.
⊥ Department of Pharmacology and Toxicology.

⊗ Abstract published in *Advance ACS Abstracts,* December 1, 1997.

[1] Abbreviations: G protein, guanine nucleotide binding protein; GTPγS, guanosine 5′-*O*-(3-thio) triphosphate; ^{125}I-BW-A844U, [^{125}I]-3-(4-amino-3-iodophenethyl)-8-cyclopentyl-1-propylxanthine; XAC, xanthine amino congener or 8-(4-((2-aminoethyl)aminocarbonylmethyl-oxy)phenyl)-1,3-dipropylxanthine; CPT, 8-cyclopentyltheophylline or 1,3-dimethyl-8-cyclopentylxanthine; ABA, N^6-(aminobenzyl)adenosine; (*R*)-PIA, (*R*)-N^6-(phenylisopropyl)adenosine; CPX, 8-cyclopentyl-1,3-dipropylxanthine; r(pHis)A_1R, hexahistidine-tagged recombinant bovine A_1 adenosine receptor; Ni^{2+}−NTA, nickel−nitrilotriacetic acid; EDC, 1-ethyl-3-(3-(dimethylamino)propyl)carbodiimide; NHS, *N*-hydroxy-succinimide; biotin BMCC, 1-biotinamido-4-[4′-(maleimidomethyl)-cyclohexanecarboxamido]butane.

S0006-2960(97)02000-X CCC: $14.00

suggests that A_1 adenosine receptors couple better to G protein heterotrimers containing γ subunits modified with a geranylgeranyl group (γ_2 and γ_3) as opposed to the farnesyl group (γ_1). A significant caveat of this approach is that Sf9 cells contain many proteins, including some endogenous G proteins (*35*, *36*), that could influence the properties of the overexpressed or reconstituted components. In the present study we have obviated these problems by using highly purified receptors and G proteins reconstituted into phospholipid vesicles to rigorously investigate the influence of the composition of the $\beta\gamma$ dimer on receptor−G protein coupling. This approach demonstrates that the nature of the G protein γ-subunit influences the ability of the A_1 adenosine receptor to bind agonists and activate guanine nucleotide exchange on the α subunit.

EXPERIMENTAL PROCEDURES

Materials. Digitonin was obtained from Gallard-Schlesinger (Carle Place, NY); phosphatidylcholine, phosphatidylserine, and cholesterol from Avanti Polar Lipids (Alabaster, AL); Ni^{2+}−NTA agarose from QIAGEN (Chatsworth, CA); heparin Sepharose CL-6B, Sephadex G-50 and Dextran 2000 from Pharmacia (Piscataway, NJ); XAC from Research Biochemicals International (Natick, MA); ABA, I-ABA, and BW-A844U were kind gifts from Dr. Susan Daluge, Glaxo-Wellcome Co. (Research Triangle Park, NC); Affigel 10, Bio-Gel P-6 DG, Amido Black 10-B, SDS, acrylamide, ammonium persulfate, TEMED, prestained molecular weight markers for SDS-PAGE from Bio-Rad (Richmond, CA); CHAPS, GTP, and GTPγS were from Boehringer Mannheim (Indianapolis, IN); dimethyl sulfoxide from Fluka (Ronkonkoma, NY); restriction enzymes from Promega Corp. (Madison, WI) or New England Biolabs Ltd. (Beverly, MA); SeaPlaque agarose from FMC (Rockland, ME); HEPES (Na^+ salt), bovine serum albumin (fraction V), phenylmethylsulfonyl fluoride, aprotinin, leupeptin, pepstatin A, benzamidine, imidazole, silver nitrate, fluorescamine, DMSO, Tween-20, EDC, and Lubrol PX from Sigma (St. Louis, MO); nitrocellulose from Schleicher and Schuell (Keene, NH); genapol C-100 from Calbiochem (San Diego, CA); biotin BMCC, streptavidin and NHS from Pierce (Rockford, IL); and [^{35}S]-GTPγS from NEN Research (Boston, MA).

Expression and Purification of Recombinant A_1 Adenosine Receptors. The construction of a recombinant baculovirus encoding the bovine A_1 adenosine receptor and its expression in Sf9 cells has been described (*1*). The bovine receptor was chosen because it binds radioligands with unusually high affinity (*1*). A modified bovine A_1 adenosine receptor with a carboxyl-terminal hexahistidine tail, r(pHis)A_1R, was engineered using PCR and the wildtype cDNA as a template. The forward primer introduced a *Sma*I site immediately 5′ to the initiation codon. The reverse primer for the r(pHis)-A_1R construct ablated the existing termination codon and inserted a hexahistidine tail, a new termination codon, and a downstream *Xba*I site. The PCR reaction was amplified for 30 cycles with the segment conditions set at 95 °C (2 min)/60 °C (1 min)/72 °C (3 min). The overhanging ends of the wildtype A_1 adenosine receptor PCR product were filled using Klenow polymerase, treated with T_4 polynucleotide kinase, and blunt-end-ligated into the *Sma*I site of pGEM7. The r(pHis)A_1R PCR product was directionally subcloned into the *Sma*I and *Xba*I sites of pGEM7. To eliminate the possibility of polymerase errors, an internal *Stu*I/*Bgl*II fragment (789 bp) was cut from the pGEM7 construct and replaced with the *Stu*I/*Bgl*II fragment from the parent clone. The resulting inserts were subcloned into the baculovirus transfer vector, pVL1393 (Invitrogen), using the *Sma*I and *Xba*I sites. To assure fidelity, the completed pVL1393 constructs were sequenced in the forward and reverse directions across the *Stu*I and *Bgl*II boundaries. The recombinant baculovirus was prepared as described (*1*).

Sf9 cells were infected with recombinant virus at a multiplicity of infection of 3:1 and incubated for 48 h. To prepare membranes, the harvested cells were thawed in 15× their wet weight of ice cold homogenization buffer, 25 mM HEPES, 100 mM NaCl, 1 mM adenosine, and protease inhibitors (100 mM phenylmethylsulfonyl fluoride, 20 mg/mL benzamidine and 2 mg/mL each of aprotinin, leupeptin, and pepstatin A) and burst by N_2 cavitation (600 psi, 20 min). Cavitated cells were centrifuged at 4 °C for 10 min at 750*g* to remove the unbroken nuclei and cell debris. The supernatant was centrifuged at 4 °C for 30 min at 28000*g*. The supernatant was discarded and the pellet was resuspended, washed twice in homogenization buffer, resuspended at a concentration of 5 mg protein/mL, snap frozen in liquid nitrogen, and stored at −70 °C.

A_1 adenosine receptors were solubilized from Sf9 cell membranes at a protein concentration of 5.0 mg/mL and a detergent to protein ratio of 4:1 (w/w). Thawed membrane pellets were washed once in 25 mM HEPES (pH 7.4), 1 mM EDTA, pelleted at 10000*g*, and resuspended in solubilization buffer containing 25 mM HEPES (pH 7.2), 1% digitonin, 1 μM adenosine, and the protease inhibitors used in the homogenization buffer. Proteins were solubilized by stirring for 2 h at 4 °C, and the extract was centrifuged at 100000*g* for 1 h. The supernatant containing detergent-solubilized receptors was applied to a 1 × 20 cm column of heparin agarose (Pharmacia) pre-equilibrated with 25 mM HEPES (pH 7.2), 0.1% digitonin, 1 μM adenosine (equilibration buffer), at a flow rate of 40 mL/h. The column was washed with ten column volumes of equilibration buffer and the receptor was eluted in a linear gradient of NaCl, 0−500 mM, in equilibration buffer. Elution fractions were assayed by binding of the antagonist ligand ^{125}I-BW-A844U (*37*), and the peak fractions were pooled and loaded onto a 1 × 5 cm column of XAC-agarose (*38*) at a flow rate of 10 mL/h. The XAC-agarose column was washed with ten volumes of equilibration buffer and the receptor eluted with ten volumes of equilibration buffer containing 100 μM CPT directly onto a 1 × 2 cm column of Ni^{2+}−NTA agarose (Qiagen) at a flow rate of 10 mL/h. The XAC-agarose/Ni^{2+}−NTA column assembly was then washed with ten column volumes of equilibration buffer containing 10 mM adenosine to remove the antagonist CPT, and the two columns were disconnected. The Ni^{2+}−NTA column was washed with twenty column volumes of equilibration buffer containing 1 mM imidazole, followed by ten column volumes of equilibration buffer containing 10 mM imidazole and the receptor eluted with 5 column volumes of equilibration buffer containing 200 mM imidazole. The elution fractions were diluted 4-fold with equilibration buffer, concentrated 20-fold by centrifugation in Centricon 30 microconcentrators (Amicon), in equilibration buffer supplemented to 10% glycerol, aliquoted, and stored at −80 °C.

Expression and Purification of Recombinant G-Protein α- and βγ-Subunits. The recombinant $G_{\alpha i2}$ subunit and several specific βγ-dimers were expressed using the baculovirus/Sf9 cell system. $G_{\alpha i2}$ was purified to homogeneity using DEAE, hydroxyapatite, and Mono P chromatography as described (*39*). The procedures used for the construction of the β and γ baculoviruses, and coexpression of the $\beta_1\gamma_1$, $\beta_1\gamma_2$, and $\beta_1\gamma_3$ dimers have been described (*40*). The βγ-subunits were purified to homogeneity by chromatography on DEAE followed by affinity chromatography on $G_{\alpha i2}$−agarose (*2*). The concentration of βγ in stock solutions was determined by quantification of silver stained gels, as described previously (*29*).

Reconstitution of r(pHis)A_1 Receptor into Phospholipid Vesicles. Phosphatidylcholine, phosphatidylserine, and cholesterol (1:1:0.1) were dispersed by sonication in a solution of 25 mM HEPES (pH 7.4), 100 mM NaCl, 1 mM EDTA, 5 mM $MgCl_2$, 1 mM DTT, and 0.5% CHAPS at a final total lipid concentration of 0.1 mg/mL. Purified adenosine receptor was added, and the mixture was then chromatographed to remove detergent on a 0.5 × 10 cm Sephadex G-50 column and eluted in 25 mM HEPES (pH 7.4), 100 mM NaCl, 1 mM EDTA, and 5 mM $MgCl_2$. The vesicles were eluted in 500 μL at the void volume of the column as determined by calibration with Dextran Blue 2000. Typically, more than 50% of the adenosine receptor added to the mixture was recovered in the phospholipid vesicles. Aliquots of vesicles containing reconstituted receptors (200 fmol ^{125}I-BW-A844U binding sites) were reconstituted with varying amounts of purified G-proteins (from 0.1−100× molar excess over r(pHis)A_1R) in a final volume of 400 μL of elution buffer and incubated for 1 h at room temperature until the start of ^{125}I-ABA binding assays.

Radioligand Binding. Radioligand binding was measured in three different preparations, Sf9 cell membranes, crude solubilized receptors, or purified receptors. The efficient detection of purified receptors required reconstitution into cell membranes lacking A_1 adenosine receptors or phospholipid rich solutions. In all cases, binding of the agonist, ^{125}I-ABA (0.1−2.5 nM), or the antagonist ^{125}I-BW-A844U (1−5 nM), to A_1 adenosine receptors was measured in binding buffer containing 10 mM HEPES (pH 7.4), 5 mM $MgCl_2$, 1 mM EDTA, and 5 units/mL adenosine deaminase with additional components noted in the figure legends in a final volume of 100 μL. Nonspecific binding of agonist was determined by the addition of 10 μM (*R*)-PIA, and nonspecific binding of antagonist was determined by the addition of 1 μM CPX. Nonspecific binding was <5% of total binding. Generally, 50 μL of radioligand in binding buffer was added to tubes containing 50 μL of membranes, crude soluble receptors, or purified reconstituted receptors. Binding assays were incubated to equilibrium for 3 h at room temperature. The binding assays were terminated by filtration over Whatman GF/C glass fiber filters (cell membranes) or GF/B filters pretreated with 0.3% (w/v) polyethyleneimine (crude and purified soluble receptors) using a Brandell Cell Harvester. The filters were rinsed thrice with 4 mL of ice-cold 10 mM Tris-Cl (pH 7.4) and 5 mM $MgCl_2$ and counted in a Wallac 1470 Wizard automatic γ counter at a counting efficiency of 75%.

^{125}I-labeling of Purified r(pHis)A_1R. To assess the degree of homogeneity of the purified receptor preparation, purifed r(pHis)A_1R preparations (and potential contaminating proteins) were radioiodinated with carrier-free $Na^{125}I$. Fifty microliters of purified r(pHis)A_1R in 25 mM HEPES, 0.1% digitonin (pH 7.2) was reacted with 200 μCi $Na^{125}I$ in the presence of 10 μL of Chloramine T (1 mg/mL) for 15 min at room temperature. Following the addition of 10 μL of $Na_2S_2O_5$ (10 mg/mL), the reaction mixtures were gel filtered by centrifugation for 5 min at 1000*g* through a 2.5 mL disposable column of Bio-Gel P-6 DG (BioRad) preequilibrated with 0.1% SDS. Typically, 10 μL of the gel-filtered iodinated receptor preparation was diluted in 5× Laemmli's buffer (*41*) and analyzed by SDS-PAGE on a 10% polyacrylamide resolving gel. The gels were soaked in 40% MeOH, 10% acetic acid, and 3% glycerol for 1 h to prevent cracking and dried on 3 MM Whatman filter paper on a slab gel dryer at 80 °C, under a vacuum, for 2 h. The dried gels were exposed to Kodak XAR film in X-ray cassettes without intensifying screens at room temperature for 1−15 min until the desired exposure was attained.

Photolabeling of A_1 Adenosine Receptors. Purified A_1 adenosine receptors were photoaffinity labeled with the antagonist ^{125}I-azido-BW-A844U by modification of the method of Patel *et al.* (*37*). In a typical reaction, 5−10 pmol of receptors (^{125}I-BW-A844U binding sites) were incubated in darkness with 5 × 10^6 cpm ^{125}I-azido-BW-A844U and 5 units/mL adenosine deaminase for 2 h at 21 °C in a final volume of 500 mL. At the end of the incubation period, the reaction mix was pipetted into a single well of a 6-well tissue culture plate (Costar), placed on ice, and exposed to ultraviolet light (Blak-Ray lamp Model XX-15) at a distance of 15 cm for 15 min. Purified photoaffinity labeled receptor was separated from the free photolabel by centrifugation for 5 min at 1000*g* through Bio-Gel P6-DG columns (BioRad) prewashed with 25 mM HEPES (pH 7.4), 50 mM NaCl, and 0.1% digitonin. Photolabeled receptors were diluted 5× into SDS prior to SDS-PAGE and autoradiography (*41*).

Deglycosylation of A_1 Adenosine Receptors. Crude soluble and affinity purified receptors were photolabeled or radioiodinated and enzmatically deglycosylated using recombinant N-glycanase (Genzyme) to hydrolyze Asn-linked oligosaccharides. A 20 μL aliquot of labeled A_1 adenosine receptor with 0.5% SDS and 50 mM β-mercaptoethanol was denatured by heating to 100 °C for 5 min. After cooling, a 10 μL aliquot of the denatured receptor was diluted to 30 μL in distilled H_2O and a final concentration of 1.25% Nonidet P-40 (Sigma). Then, 0.5 U of N-glycanase was added, and the reaction mixture was incubated for 18 h at 37 °C. The reaction was terminated by a 5-fold dilution into SDS prior to SDS-PAGE and autoradiography (*41*).

Assay of [^{35}S]-GTPγS Binding. [^{35}S]-GTPγS binding to G-protein α subunits was assessed by a modification of the method of Liang and Garrison (*42*). Phospholipid vesicles containing r(pHis)A_1 receptors were eluted from gel filtration columns in 25 mM HEPES (pH 7.4), 100 mM NaCl, 1 mM EDTA, and 5 mM $MgCl_2$ and diluted to a receptor concentration of about 25 fmol ^{125}I-BW-A844U binding sites/100 μL. Following the addition of 1 mM DTT, 10 nM GDP, and 5 units/mL adenosine deaminase, G-protein subunits were added, and the mixture was incubated for 15 min on ice. Nucleotide exchange was initiated with 0.1 volume of elution buffer containing 2 × 10^6 dpm [^{35}S]-GTPγS/mL (3 nM) and 10 μM (*R*)-PIA and continued at 22 °C for 10 min. Nonspecific binding was determined by adding 100 μM unlabeled GTPγS. At the end of the incubation period, the

reaction was terminated by adding 3 mL of cold wash buffer (10 mM Tris, pH 7.4, 1 mM $MgCl_2$). Bound and free ligand were separated by filtration through BA85 0.45 μM nitrocellulose filters (Schleicher and Schuell). Free ligand was removed by washing three times with 3 mL of cold wash buffer. Filters were immersed in 5 mL of Ready Safe liquid scintillation cocktail (Beckman), and the [^{35}S]-GTPγS retained on the filters was counted in a liquid scintillation counter at a counting efficiency of 70%.

Monitoring the Interaction between $\beta\gamma$ Subunits and Immobilized $G_{\alpha i2}$ Using the IAsys Optical Biosensor. Recombinant $G_{\alpha i2}$ was immobilized on the IAsys optical biosensor cuvette by exploiting the extremely tight binding of biotin to streptavidin. This strategy was chosen because biotinylated α subunits retain their ability to bind $\beta\gamma$ (*43*), streptavidin coupled to carboxymethyldextran still binds biotin with high affinity (IASys Cuvette SystemMethods Guide), and the streptavidin-biotin link should present minimal hindrance to the α-$\beta\gamma$ interaction. Purified recombinant $G_{\alpha i2}$ subunits in storage buffer (50 mM Hepes, pH 8.0, 1 mM EGTA, 1 mM DTT, 10 μM GDP, 5 mM $MgCl_2$) were supplemented to 5 mM DTT and incubated for 30 min at 4 °C. The DTT was removed by gel filtration over BioGel P6-GD columns (1 × 3 cm), prewashed by centrifugation for 10 min at 1000*g* in biotinylation buffer (60 mM NaPi, pH 7.6, 150 mM NaCl, 0.05% Genapol C-100, 2 mM $MgCl_2$, 5 μM GDP). The pass-through containing the $G_{\alpha i2}$ was collected. Biotin-BMCC was dissolved in DMSO at a concentration of 60 μM immediately before use and diluted 1/10 into the pass-through to give a final concentration of 6 μM biotin-BMCC and approximately 10 μM $G_{\alpha i2}$. This mixture was allowed to react at room temperature for 10 min. The reaction was stopped by loading the mixture onto a freshly prepared spin column equilibrated in biotinylation buffer and centrifuging as described above. The eluate from the spin column containing biotinylated $G_{\alpha i2}$ was stored on ice until coupled to strepavidin (see below).

Streptavidin was immobilized on a carboxymethyldextran cuvette (Affinity Sensors) by amine coupling according to the manufacturer's instructions. Briefly, the cuvette was installed in the IAsys optical biosensor system (Affinity Sensors, Paramus, NJ) and equilibrated with 200 μL of PBS/T (0.01 M NaP_i, pH 7.4, 2.7 mM KCl, 0.137 M NaCl, 0.05% Tween 20) for 10 min. The carboxymethyl dextran matrix was activated by treatment with a freshly prepared mixture of 0.4 M EDC and 0.1 M NHS for 8 min at 25 °C. The cuvette was washed three times with PBS/T and finally loaded with 200 μL of 10 mM NaAc, pH 4.5. The streptavidin stock solution (1 mg/mL in borate saline, pH 7.8, 0.02% NaN_3) was diluted 1:20 into the activated cuvette to a final concentration of 50 μg/mL streptavidin. The coupling reaction was allowed to proceed for 10 min. The streptavidin solution was removed and the cuvette washed with PBS/T for 2 min. The remaining esters were reacted with 1 M ethanolamine, 10 mM Na borate, pH 8.5, for 2 min. The streptavidin cuvette was washed several times with PBS/T until a steady baseline was obtained and then washed three times with biotinylation buffer, emptied, and the freshly biotinylated $G_{\alpha i2}$ solution was introduced. After 10 min the cuvette was emptied and washed twice with biotinylation buffer. Binding is measured in units of arc-seconds (arc-s). On the basis of a calibration curve constructed with human serum albumin, 163 arc-s corresponds to binding of 1 ng/mm^2 (IAsys Cuvette System Methods Guide). Approximately 500 arc-s of streptavidin and 500 arc-s of $G_{\alpha i2}$ were immobilized. The cuvette was stored in $\beta\gamma$ binding buffer (20 mM Hepes, pH 8, 1 mM EDTA, 200 mM NaCl, 0.6% CHAPS, 5 mM $MgCl_2$, 5 μM GDP, 1 mM DTT) at 4 °C.

Measurement of $\beta\gamma$ Binding to Immobilized, Biotinylated $G_{\alpha i2}$. The $G_{\alpha i2}$ cuvette was equilibrated with $\beta\gamma$ binding buffer at 25 °C until a stable baseline was obtained. Binding was initiated by dilution of a concentrated stock of $\beta\gamma$ in binding buffer into a known volume of binding buffer in the cuvette, typically 5−25 μL concentrated $\beta\gamma$ stock into 125−175 μL $\beta\gamma$ binding buffer. Association data were collected for 200−300 s. Dissociation was initiated by removal of the $\beta\gamma$ solution and replacement with fresh $\beta\gamma$ binding buffer. Dissociation data were collected for 200−300 s. The cuvette was then washed several times with $\beta\gamma$ binding buffer until the baseline stabilized. Two controls were performed. Streptavidin was immobilized to a carboxymethyl dextran cuvette via EDC/NHS chemistry as described above and then washed several times with $\beta\gamma$ binding buffer. A stable baseline was obtained, and a concentrated aliquot of $\beta\gamma$ in binding buffer added to a final concentration of 100 nM $\beta\gamma$. No binding was observed. For the second control, a $G_{\alpha i2}$ derivatized cuvette was equilibrated with buffer designed to activate the α subunit ($\beta\gamma$ binding buffer plus 10 mM NaF, 30 μM $AlCl_3$, 50 mM $MgCl_2$). Equilibration with activation buffer resulted in a steep (100 arc-s/min) but reversible baseline slope. A concentrated aliquot of $\beta\gamma$ stock was added, and no binding was observed under these conditions.

Calculation of G-Protein α and $\beta\gamma$ Affinity. Curve fitting was performed with IAsys Fastfit software. Raw association data was fit with a single phase exponential which was then used to calculate maximal binding (extent in Figure 6). The dependence of extent on the concentration of $\beta\gamma$ was fit by a rectangular hyperbola to determine K_{Deq}. The association rate constant, k_a, was calculated from the slope of a plot of k_{on} (derived from the single phase exponential fit of the association data) vs the concentration of $\beta\gamma$. Dissociation rate constants were calculated either by a fit of experimental data to a single exponential, or by calculating the intercept of a plot of k_{on} vs [$\beta\gamma$].

Data Analysis. The figures shown in the results are typical of two or more replicate experiments of the same or similar experimental design. Averaged data are presented as means ±SEM. Curve fitting was done by Marquardt's nonlinear least squares method (*44*). Models which best fit the data were chosen based on the method of Motulsky and Ransnas (*45*).

RESULTS

Purification of Recombinant A_1 Adenosine Receptors. Solubilization of the r(pHis)A_1R under conditions optimal for the preservation of radioligand binding was achieved using digitonin. At a detergent to protein ratio of 4:1 (w/w), CHAPS, *n*-octyl glucoside, lubrol PX, cholate, and dodecyl-β-maltoside all were found to be less effective than digitonin in solubilizing receptors that retained the ability to bind the radioligand, ^{125}I-BW-A844U (data not shown). The recovery and purification of functional receptors through four steps of purification is summarized in Figure 1 and Table 1. The first step, heparin−sepharose affinity chromatogra-

Table 1: Purification of r(pHis)A_1R from Sf9 Cell Membranes. Data Are Derived from a Single Purification and Are Representative of Three Similar Experiments. The Values Varied Less Than 25% for All Steps

step	total activity,[a] pmol	total protein, mg	specific activity, pmol/mg	yield, %	purification factor, *n*-fold
Sf9 cell membranes	548	458	1.19	100	1
digitonin-solubilized	205	104	1.98	37.5	1.7
heparin−sepharose	114	25.2	4.52	20.8	3.8
XAC-agarose/Ni^{2+}−NTA	11.8	0.0013	9080	2.2	7630

[a] Binding activities were assessed using 5 nM ^{125}I-BW-A844U as described under Experimental Procedures.

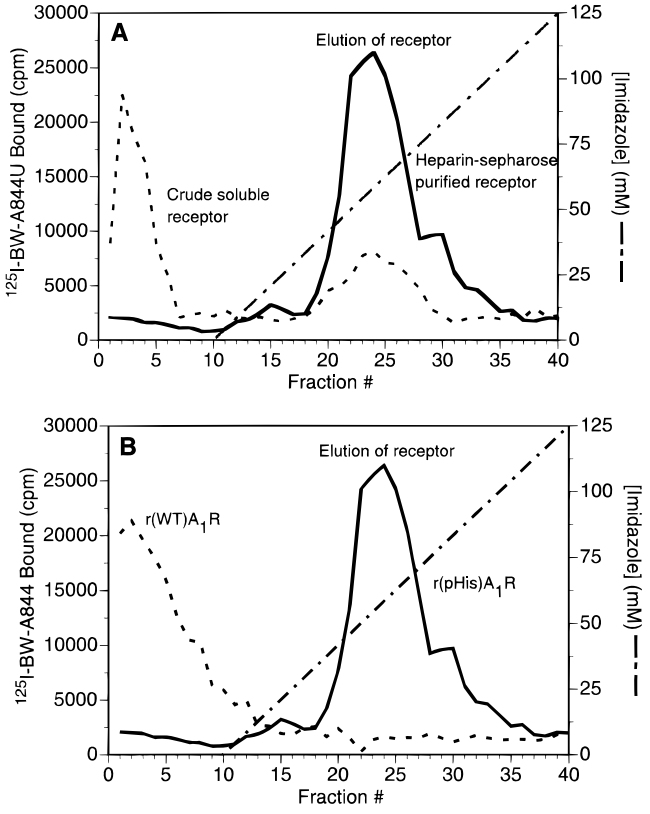

FIGURE 1: Chromatography of r(pHis)A_1 receptor on heparin−sepharose and Ni^{2+}−NTA agarose. (A) Partial purification of r(pHis)A_1R by heparin−sepharose chromatography enhances the binding of r(pHis)A_1R to Ni^{2+}−NTA agarose. The elution profile of ^{125}I-BW-A844U binding activity from a Ni^{2+}−NTA agarose column is shown for preparations of receptor solubilized from Sf9 cell membranes (- - -) and preparations partially purified by heparin−sepharose chromatography (—) as described under Experimental Procedures. Identical amounts of ^{125}I-BW-A844U binding sites from crude soluble and heparin−sepharose purified r(pHis)A_1R were diluted to 10 mL in 25 mM Hepes, 100 mM NaCl, 0.1% digitonin (pH 7.4) and applied to 1 mL of Ni^{2+}−NTA columns equilibrated with the same buffer at a flow rate of 20 mL/h. (B) Specificity of Ni^{2+}−NTA affinity chromatography for r(pHis)A_1R. The retention and elution patterns are shown for preparations of r(wt)A_1R (- - -) and r(pHis)A_1R (—) following partial purification over heparin sepharose columns. Following sample application, the Ni^{2+}−NTA columns were washed with 10 mL of equilibration buffer and then eluted in a 60 mL of linear gradient of equilibration buffer containin 0−125 mM imidazole. Two milliliter fractions were collected and assayed for ^{125}I-BW-A844U binding.

phy, resulted in only a small (2.3-fold) purification, but substantially improved the recovery of receptors in the subsequent purification step, regardless of whether the next step was XAC-agarose or Ni^{2+}−NTA affinity chromatography. This finding is illustrated in Figure 1A which shows the retention and elution of r(pHis)A_1R from Ni^{2+}−NTA columns without (dotted line) or with (solid line) prior partial purification over heparin−sepharose. The recombinant bovine A_1 adenosine receptor without the hexahistidine extension did not adhere to Ni^{2+}−NTA columns (dotted line, Figure 1B). This is consistent with the expectation that the site of interaction between r(pHis)A_1R and Ni^{2+} is the hexahistidine moiety added to the carboxyl terminus of r(pHis)A_1R.

The combined use of heparin sepharose and Ni^{2+}−NTA resulted in only a 300−400 fold purification of the r(pHis)-A_1R (data not shown). To achieve greater purification, a XAC-agarose affinity chromatography step was added prior to the Ni^{2+}−NTA step. The XAC-agarose step greatly increased the degree of purification. Ni^{2+}−NTA chromatography was still useful as a last step because it served to concentrate receptors that were slowly eluted from the XAC-agarose columns, it removed the cyclopentyltheophylline used to elute the receptor, and it afforded an extra degree of purification. The best results were achieved when the eluate of the XAC-agarose column was applied directly to the Ni^{2+}−NTA column, hence data representing these two steps are combined in Table 1.

Recombinant adenosine receptors were purified from infected Sf9 cell membranes to a specific binding activity of 12.3 nmol/mg protein (Figure 2A). This represents 45% of the theoretical number of binding sites for a homogeneous 36 kDa protein, 27 nmol/mg protein. The K_D of the antagonist radioligand, ^{125}I-BW-A844U, for binding to r(pHis)A_1R on Sf9 cells membranes, 0.48 ± 0.09 nM, did not differ significantly from the K_D for binding to purified receptors, 0.52 ± 0.16 nM, and is similar to the K_D noted previously for native receptors in bovine brain membranes and recombinant receptors in Sf9 cell membranes (*1,37*).

When purified receptors were concentrated so that they could be visualized by silver staining, they aggregated. The aggregation was increased by boiling receptors in SDS. Consequently, radioiodination of unconcentrated receptors that were not boiled prior to electrophoresis was used as an alternative means of visualization (Figure 2B). Following poylacrylamide gel electrophoresis, the purified radioiodinated receptor was observed as a 36 kDa protein (*lanes 1 and 2*). Since no other radioiodinated proteins were visible, the receptor preparation appears to be homogeneous. A protein of identical molecular mass is seen if purified receptors are photoaffinity labeled with ^{125}I-azido-BW-A844U (*lane 3*). Upon deglycosylation with *N*-glycanase, the 36 kDa band shifts to 34 kDa (*lane 4*). This result was not observed if the *N*-glycanase was denatured (*lane 5*).

Figure 3 shows competition by the agonist, (*R*)-PIA, for binding by the antagonist radioligand, ^{125}I-BW-A844U, to r(pHis)A_1R in Sf9 cell membranes and to purified receptors reconstituted into a lipid rich suspension. As we have noted previously (*1*), recombinant receptors overexpressed in Sf9

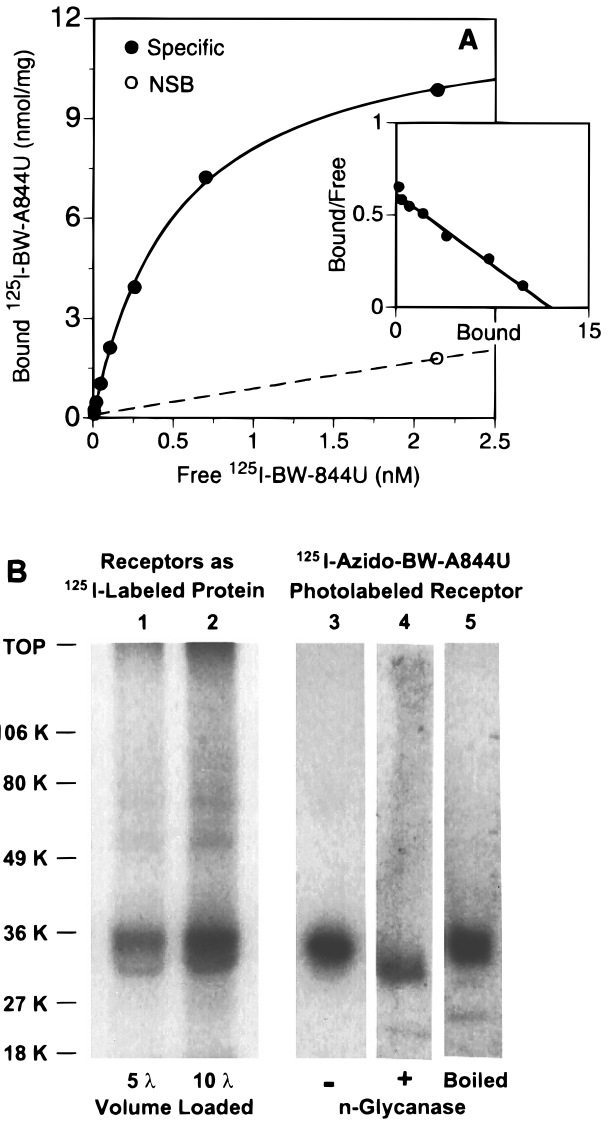

FIGURE 2: Characterization of purified r(pHis)A_1R by ^{125}I-BW-A844U binding and SDS-PAGE. (A) A saturation isotherm of ^{125}I-BW-A844U binding to fully purified r(pHis)A_1R was performed. Purified receptor (1.5 ng) was reconstituted into COS cell membranes (100 μg/200 μL) and assayed with varying concentrations of ^{125}I-BW-A844U and the data fit to a single site binding equation. The K_D and B_{max} values are 0.52 ± 0.16 nM and 12.3 ± 3.75 nmol/mg protein, respectively. The inset is a Scatchard plot. Each point is the mean of triplicate determinations. Standard error bars are smaller than the symbols. Similar results were obtained in a duplicate experiment. (B) Autoradiogram of radioiodinated (lanes 1 and 2) or photolabeled (lanes 3−5) aliquots of purified r(pHis)-A_1R following SDS-PAGE. Total protein from pooled purified fractions from a typical purification was radioiodinated or photolabeled as described under Experimental Procedures. Lane 1 and lane 2 show ^{125}I-labeled total protein from a purified fraction. Aliquots of purified receptors photolabeled with ^{125}I-BW-A844U (lane 3) were enzymatically deglycosylated with N-glycanase (lane 4). Control samples were treated with boiled N-glycanase (lane 5).

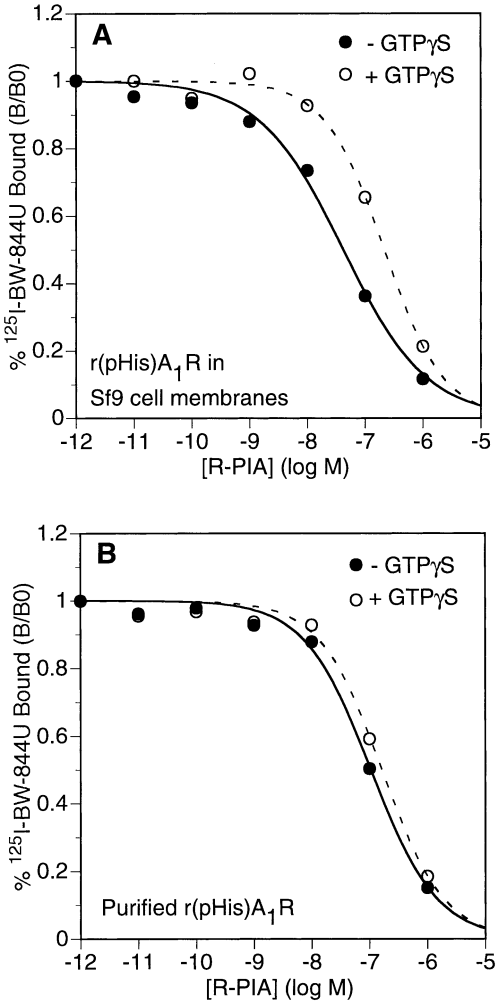

FIGURE 3: Effect of guanine nucleotides on agonist binding to Sf9 cell membranes expressing r(pHis)A_1 receptors or to purified r(pHis)A_1 receptors. Competition by (*R*)-PIA for ^{125}I-BW-A844U binding was determined in the presence of 0.5 nM ^{125}I-BW-A844U and various concentrations of (*R*)-PIA for 3 h at 23 °C with Sf9 cell membranes expressing the r(pHis)A_1R (panel A), or purified r(pHis)A_1R (panel B). The experiments were performed in the presence or absence of 100 μM GTPγS. For the assay of the purified receptor, r(pHis)A_1R was diluted into 50 μL aliquots of the lipid rich pass-through fractions from the heparin column (25 μg protein) which had been heated to 80 °C for 3 min to inactivate G proteins and desalted into binding buffer. Total binding of the membrane-bound and purified receptor preparations was 55000 cpm and 45000 cpm, respectively. The data are representative of two independent experiments.

cell membranes are partially coupled to G proteins. As expected, GTPγS causes a rightward shift in the agonist concentration response curve, increasing the IC_{50} from 67 nM to 212 nM. This is accompanied by an increase in the Hill coefficient (N_h) from 0.5 to 0.85. This shift can be attributed to the loss of high affinity agonist binding sites (Figure 3A). In contrast, (*R*)-PIA binds with only low affinity to the purified r(pHis)A_1R (IC_{50} = 160 nM and N_h = 0.81) and is not affected by the addition of GTPγS (Figure 3B), indicating that G proteins are not co-purified with receptors. Overall, the data shown in Figures 1−3 and Table 1 demonstrate that the A_1 adenosine receptors are highly purified, free of G proteins, and bind ^{125}I-BW-A844U and (*R*)-PIA with the same low affinity as uncoupled receptors expressed in plasma membranes.

Reconstitution of Purified r(pHis)A_1 Adenosine Receptors with G Proteins. We next examined the interaction of the purified r(pHis)A_1R reconstituted into phospholipid vesicles with recombinant G proteins of defined composition. The ability of G proteins to increase high affinity agonist binding to the receptor was dependent on the nature of the γ subunit in the $\beta\gamma$ dimer as shown in Figure 4. The time courses of agonist binding to receptors reconstituted with G protein complexes containing β_1 and either γ_1 or γ_3 are shown in Figure 4A. In this experiment, the ratio of A_1R:α:$\beta\gamma$ was 1:1:5. At equilibrium, binding of ^{125}I-ABA to receptor−G

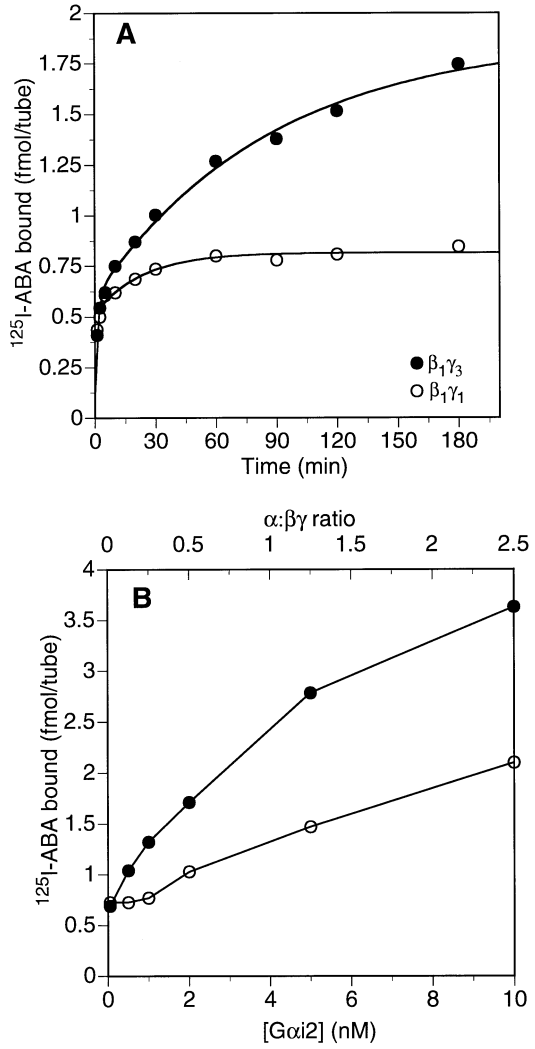

FIGURE 4: The effect of G protein $\beta\gamma$ subunit composition on agonist binding to purified r(pHis)A_1R. (A) Time courses of specific agonist binding to r(pHis)A_1 adenosine receptors reconstituted into lipid vesicles is shown for: $\beta_1\gamma_1$ and $\beta_1\gamma_3$ with the ratio of A_1R:α:$\beta\gamma$ = 1:1:5. The concentrations of $G_{\alpha i2}$ and r(pHis)A_1R were fixed at 0.5 nM in a 1:1 ratio. Binding was performed as indicated under Experimental Procedures. Data were optimally fit to bi-exponential curves. (B) Changes in the maximal specific binding of ^{125}I-ABA to the r(pHis)A_1 adenosine receptor with varying concentrations of $G_{\alpha i2}$. r(pHis)A_1R concentration was fixed at 0.6 nM, $\beta\gamma$ at 4 nM and radioligand at 1 nM. The α subunit concentration was varied between 0 and 10 nM. Equilibrium binding was determined as described under Experimental Procedures. These experiments are representative of four other experiments of similar design.

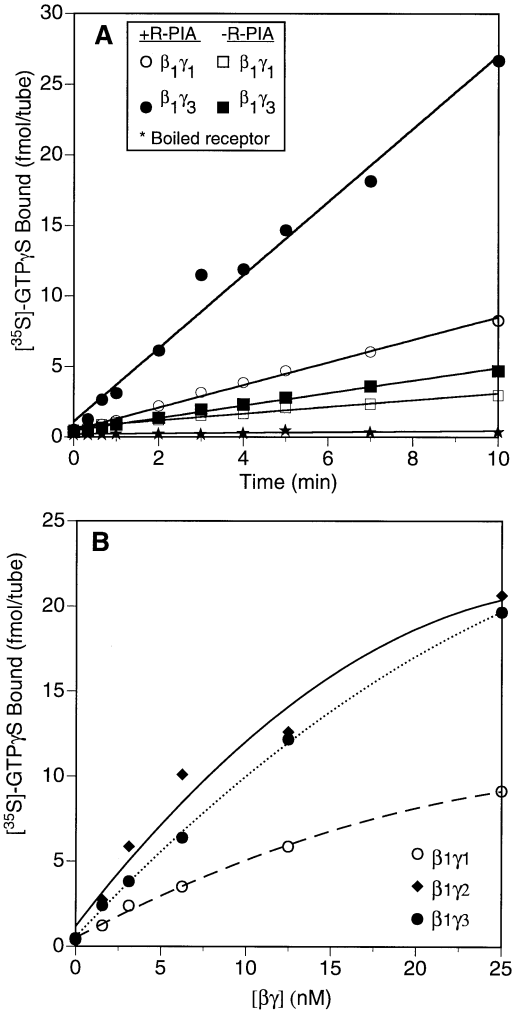

FIGURE 5: Effect of $\beta_1\gamma_1$ and $\beta_1\gamma_3$ on r(pHis)A_1 receptor -catalyzed GTPγS exchange on $G_{\alpha i2}$. (A) The time course of r(pHis)A_1R-catalyzed [^{35}S]-GTPγS specific binding to $G_{\alpha i2}$ was measured utilizing the indicated reagent conditions. Reactions were carried out at 23 °C using 6.6 nM $G_{\alpha i2}$, 6.6 nM $\beta\gamma$, and 0.24 nM purified r(pHis)A_1R. The [^{35}S]-GTPγS concentration was 1.5 nM. Control experiments performed in the absence of $\beta\gamma$ or receptors gave results similar to boiled receptors (not shown). These experiments are representative of four other experiments of similar design. (B) The effect of increasing concentrations of recombinant $\beta\gamma$ dimers on r(pHis)A_1R-catalyzed specific binding of [^{35}S]-GTPγS to $G_{\alpha i2}$. Reactions were carried out for 5 min at 23 °C using 1.66 nM $G_{\alpha i2}$, 1.66 nM $\beta\gamma$, and 0.1 nM purified r(pHis)A_1R. Control experiments were performed in the absence of $\beta\gamma$ complex. Nonspecific binding was determined in the presence of 100 μM GTPγS. Individual points are the means of duplicate determinations from a representative experiment repeated twice.

protein complexes containing $\beta_1\gamma_3$ is about 2.5 fold higher than to complexes containing $\beta_1\gamma_1$. There are two kinetic components of ligand binding and the increased binding induced by $\beta_1\gamma_3$ appears to be due to the slower component. The slow components probably reflect the rates of formation of L-*R-α-$\beta\gamma$ complexes, where R* denotes receptors that bind agonist with high affinity. Figure 4B shows the influence of $\beta\gamma$ composition on high-affinity ^{125}I-ABA binding to *R as a function of $G_{\alpha i2}$ subunit concentration. Binding to receptor−G protein complexes containing the $\beta_1\gamma_3$ dimer exceeds binding to complexes containing $\beta_1\gamma_1$ by approximately 2-fold and this difference is independent of the $G_{\alpha i2}$ concentration.

Guanine Nucleotide Binding to Reconstituted r(pHis)-A_1R-G Protein Complexes. Using the reconstituted vesicle system, we next determined if the changes in agonist binding in response to altering the $\beta\gamma$ subunit composition are associated with differences in the ability of an agonist to increase the rate of [^{35}S]-GTPγS binding. Figure 5A shows [^{35}S]-GTPγS binding to $G_{\alpha i2}$ in the presence of an equimolar concentration of purified recombinant $\beta_1\gamma_1$ or $\beta_1\gamma_3$. Lipid vesicles containing receptor and G-protein subunits were incubated together for 15 min on ice and the assay was initiated by the addition of [^{35}S]-GTPγS and 10 μM (*R*)-PIA. Agonist-induced guanine nucleotide exchange, estimated as the rate of [^{35}S]-GTPγS binding measured in the presence of GDP, was linear over 10 min. No effect of agonist was observed in the absence of either the α or the $\beta\gamma$ subunit or in control reactions containing heat-denatured receptors. In the absence of agonist-stimulation (*squares*)

the addition of receptor to α and $\beta\gamma$ subunits produced only a small constitutive increase in GTPγS binding to $G_{\alpha i2}$ which proceeded at a slightly faster rate with the $\beta_1\gamma_3$ than the $\beta_1\gamma_1$ dimer. Agonist-stimulated [^{35}S]-GTPγS binding (*circles*) was increased by both recombinant $\beta\gamma$ dimers tested, but to different degrees. In the presence of the $\beta_1\gamma_3$ dimer, [^{35}S]-GTPγS binding was increased approximately 6-fold, while $\beta_1\gamma_1$ only supported a 3-fold increase. Figure 5B shows the concentration-dependence of the ability of three different recombinant $\beta\gamma$ dimers to support guanine nucleotide exchange. Over the range of concentrations chosen, receptor−G protein complexes containing the γ_1 subunit exhibited a 2-fold lower rate of [^{35}S]-GTPγS binding to $G_{\alpha i2}$ compared to complexes containing either γ_2 or γ_3 subunits. The magnitude of the difference is approximately the same over a wide range of α:$\beta\gamma$ concentration ratios. Considered together, the data in Figures 4 and 5 suggest that the γ subunit composition can affect the conformation of receptors and α-subunits in receptor−G protein complexes.

Determination of the Affinity of the α-$\beta\gamma$ Interaction. Differences in the affinity of the α subunit for $\beta\gamma$ subunits could account for the results observed in Figures 4 and 5. To investigate this directly, we used an optical biosensor to monitor the interaction between recombinant $\beta\gamma$ subunits and recombinant $G_{\alpha i2}$ immobilized on the biosensor cuvette. This technique utilizes a resonant mirror to detect increases in refractive index due to binding of proteins free in solution to the immobilized protein on the cuvette surface (*46*). For globular proteins, a linear relationship exists between the mass of the protein bound to the surface and the change in refractive index measured in arc-seconds. Both the affinities and kinetics of protein−protein interactions may be determined. Biotinylated $G_{\alpha i2}$ was first immobilized on streptavidin coated cuvettes, and then highly purified, recombinant $\beta_1\gamma_1$ or $\beta_1\gamma_2$ dimers were introduced in solution.[2] The equilibrium K_D of this interaction was calculated by plotting the extent (maximal binding) in units of arc seconds versus $\beta\gamma$ concentration and fitting these data to a rectangular hyperbola as shown in Figure 6A. Table 2 summarizes the binding parameters. The K_{Deq} of the two $\beta\gamma$ subunits is not significantly different as judged by the unpaired t test. Therefore, the data for both $\beta\gamma$ dimers was combined and analyzed as one data set. The K_{Deq} calculated for the combined data was 112 ± 37 nM. In order to calculate a K_D value based on kinetics (k_d/k_a), we measured the rate of dissociation of $\beta\gamma$ from immobilized α_{i2}. Figure 6B shows representative dissociation curves for $\beta_1\gamma_1$ and $\beta_1\gamma_2$ and the calculated k_{off} values are listed in Table 2. This experiment illustrates that both $\beta\gamma$ dimers dissociate at similar rates. The K_D calculated from k_d/k_a is consistent with the values calculated from the equilibrium measurements.

Determinations of protein interactions involving an immobilized partner are nonideal and subject to practical complexities. Two tests may be applied to the kinetic results to verify self-consistency (*47*). The first consistency test requires that K_D calculated for the dependence of extent of binding on [$\beta\gamma$] be in agreement with the K_D calculated from the ratio of the kinetics constants, k_d/k_a. As shown in Table 2, our K_{Deq} is within a factor of 2−3 of K_{Dkin}. The second test requires that the direct determination of k_{off} be approximately equal to that calculated from the slope of the linear regression of k_{on} vs [$\beta\gamma$]. The data sets for both $\beta_1\gamma_1$ and $\beta_1\gamma_2$ satisfy this requirement. Our determination of K_D is in qualitative agreement with previous determinations of α-$\beta\gamma$ affinity. Using a variety of techniques and quite different buffers and detergents, the K_D has been observed to range from about 1 nM to 300 nM (*31*,*48*−50). Our determination of K_D's of 112 nM using recombinant proteins falls within the range of these previous determinations and supports the hypothesis that the γ subunit in the $\beta\gamma$ dimer does not affect the affinity of the interaction between the α_{i2} and β_1 subunits in the absence of receptor.

Influence of the $\beta\gamma$ Composition on the Dissociation Rate of Bound Agonist. On the basis of the results presented above, we reasoned that variations in guanine nucleotide

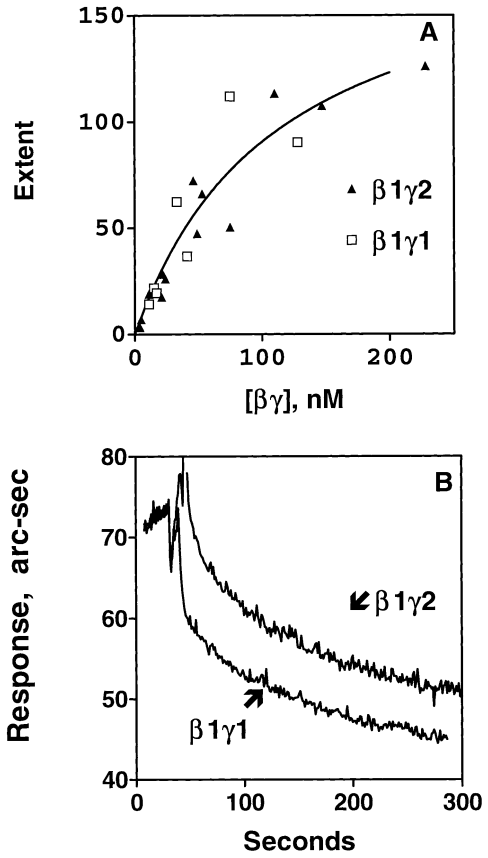

FIGURE 6: Effect of $\beta\gamma$ composition on the affinity of the interaction between α and $\beta\gamma$ subunits. (A) Equilibrium binding of purified recombinant $\beta\gamma$ to immobilized biotinylated $G_{\alpha i2}$. Binding was measured for $\beta_1\gamma_1$ (□) and $\beta_1\gamma_2$ (▲). Extent of binding was calculated for each $\beta\gamma$ concentration based on an exponential fit of the association data for the first 200 s of binding. The K_D calculated from the $\beta_1\gamma_1$ data is not statistically different from that calculated for $\beta_1\gamma_2$. Dissociation rate constants calculated from the intercept of a plot of k_{on} vs [$\beta\gamma$] are in agreement with the direct determinations. Each data point was derived from a separate experiment. (B) A typical experiment showing the kinetics of dissociation of $\beta_1\gamma_1$ and $\beta_1\gamma_2$ from immobilized α_{i2}. After approximately 300 s of binding, dissociation was initiated by removal of free $\beta\gamma$ and replacement with fresh $\beta\gamma$ binding buffer (20 mM HEPES, pH 8.0, 1 mM EDTA, 200 mM NaCl, 0.6% CHAPS, 5 mM $MgCl_2$, 5 mM GDP, and 1 mM DTT). The dissociation rate constant was calculated by fitting a single phase exponential to approximately 200 s of data.

[2] The $\beta_1\gamma_2$ dimer was used for comparison with $\beta_1\gamma_1$ in these experiments because it was available in higher concentration than $\beta_1\gamma_3$. This substitution appears justified as the γ_2 protein is 89% similar to $\gamma_3\gamma_3$ in amino acid composition, has the same geranylgeranyl group at its carboxyl terminus, and the $\beta_1\gamma_2$ dimer is functionally similar in assays of adenosine receptor coupling and effector activation (Figure 5B and references (*1*−*3*)).

Table 2: Binding Parameters for $G_{\alpha i2}$ and $\beta\gamma$ Interactions Measured Using an Optical Biosensor As Described in Experimental Procedures

	k_{off},[a] s^{-1}, mean ± SE (*n*)	k_a,[b] M^{-1} s^{-1}, mean ± SE (*n*)	K_{Deq},[c] nM, mean ± SE	K_{Dkin},[d] nM
$\beta_1\gamma_1$	0.012 ± 0.001 (10)	44,000 ± 6,600 (12)	85 ± 70	271
$\beta_1\gamma_2$	0.008 ± 0.001 (10)	34,000 ± 1,200 (8)	134 ± 47	233
combined data	−	−	112 ± 37	−

[a] Direct determination. May also be determined from the *y*-intercept of the plot of k_{on} vs [$\beta\gamma$]: $\beta_1\gamma_1$, 0.010; $\beta_1\gamma_2$, 0.005. [b] Calculated from the slope of k_{on} vs [$\beta\gamma$]. [c] Calculated from plot of extent vs [$\beta\gamma$] (Figure 6A). [d] Calculated from $K_D = k_d/k_a$.

exchange rates observed among $\beta\gamma$ dimers might be associated with a change in the conformation of the receptor in the L-A_1*R-α-$\beta\gamma$ complex. To explore this possibility, ^{125}I-ABA was incubated to equilibrium with receptor−G protein vesicles and the time course of radioligand dissociation was assayed following the addition of a large excess of unlabeled agonist to the system. Figure 7A shows the kinetics of dissociation of ^{125}I-ABA from low- and high-affinity r(pHis)-A_1R binding sites in the presence of α_{i2} and either $\beta_1\gamma_1$ or $\beta_1\gamma_3$. Pooled data were fit to mono- or biexponential equations. As expected, the addition of 100 μM GTPγS caused a rapid dissociation of radioligand, presumably by converting most receptors to the low affinity uncoupled conformation (*squares*). In the absence of GTPγS (*circles*), a high affinity, slowly dissociating component of binding is apparent. The half-time ($t_{1/2}$) for agonist dissociation from the high affinity binding sites containing the two $\beta\gamma$ subunits differs significantly, 8.45 ± 1.65 min in the presence of $\beta_1\gamma_1$ and 16.5 ± 4.7 min in the presence of $\beta_1\gamma_3$ ($p < 0.01$). The difference in the dissociation rate of the slow component is more easily seen in Figure 7B, a semilogarithmic plot of high affinity (GTPγS-sensitive) ^{125}I-ABA binding vs time. These data are fit by straight lines with slopes equal to $-k_{diss}$ for radioligand binding to G protein coupled receptors. Thus, the affinity of ligand binding to the A_1*R-α-$\beta\gamma$ complex depends on the identity of the $\beta\gamma$ dimer.

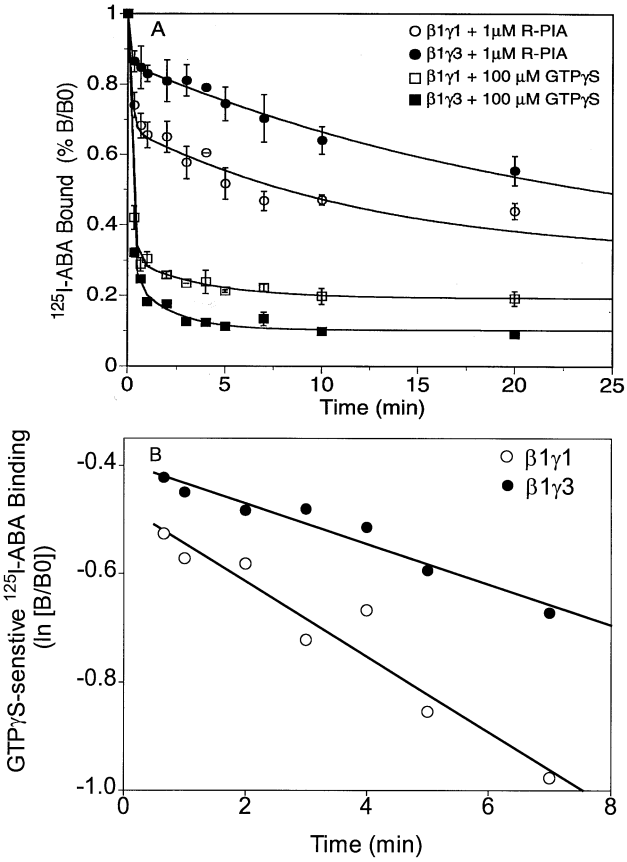

FIGURE 7: The effect of $\beta\gamma$ subunit composition on the dissociation of ^{125}I-ABA from r(pHis)A_1 adenosine receptors reconstituted into phospholipid vesicles. ^{125}I-ABA (0.45 nM) was allowed to bind to reconstituted receptors (0.5 nM), $G_{\alpha i2}$ (0.5 nM), and various $\beta\gamma$ subunits (2.5 nM) at 23 °C until equilibrium was reached. Total binding at equilibrium was approximately 1.5-fold higher for $\beta_1\gamma_3$ than for $\beta_1\gamma_1$. At time zero, 1 μM unlabeled I-ABA was added, and aliquots were removed at the indicated times and filtered as described in Methods. Low affinity binding was determined by adding 100 μM GTPγS and I-ABA at time 0. (A) Untransformed binding data. Each point is the mean ±SE of two closely agreeing independent experiments, each assayed in triplicate. The dissociation rates in the absence of GTPγS (circles) are fit significantly better to bi- than to monoexponential equations ($P < 0.001$). (B) Semilogarithmic plot of ^{125}I-ABA binding to G protein coupled receptors. The binding measured in the presence of GTPγS at 20 min (as shown in A) was subtracted from total binding at each time pont. The natural logarithm of these data, excluding early time points (<0.5 min, low affinity binding) is plotted vs time. The slopes of these lines, defining $-k_{diss}$ of the radioligand from G protein coupled receptors, are −0.0697 and −0.0375 min^{-1} for $\beta_1\gamma_1$ and $\beta_1\gamma_3$, respectively.

DISCUSSION

The current work examined in detail the influence of G protein $\beta\gamma$ composition on the ability of the A_1 adenosine receptor to activate guanine nucleotide exchange and to bind an agonist, ^{125}I-ABA. Since experiments were performed using highly purified, recombinant receptors and three purified G protein heterotrimers reconstituted into lipid vesicles, the results can unequivocally be attributed to protein−protein interactions. A novel and effective method for purifying hexahistidine-tagged A_1 adenosine receptors was developed which can potentially be adapted as a general method for purification of hexahistidine-tagged receptors. It is notable that heparin−sepharose chromatography markedly improved the purification of the hexahistidine-tagged receptor by subsequent Ni^{2+}−NTA affinity chromatography (Figure 1A). Ni^{2+}−NTA affinity chromatography alone only partially purified receptors, and it was necessary to combine this procedure with ligand affinity chromatography to purify receptors to near homogeneity.

The purified A_1 adenosine receptor binds ligands with the same affinity as the native receptor and couples efficiently to pure, recombinant G protein heterotrimers. The identity of the G protein $\beta\gamma$ dimer does not affect its interaction with $G_{\alpha i2}$ measured in the absence of receptor (Figure 6) but does influence A_1 receptor coupling as judged by agonist-stimulated guanine nucleotide exchange on the G protein α subunit and agonist binding. Heterotrimers containing the $\beta_1\gamma_2$ or $\beta_1\gamma_3$ dimer display greater agonist-stimulated guanine nucleotide exchange and bind ^{125}I-ABA with higher affinity than complexes containing the $\beta_1\gamma_1$ dimer. Overall, the data are consistent with the hypothesis that the nature of the γ subunit is an important determinant of the interaction between

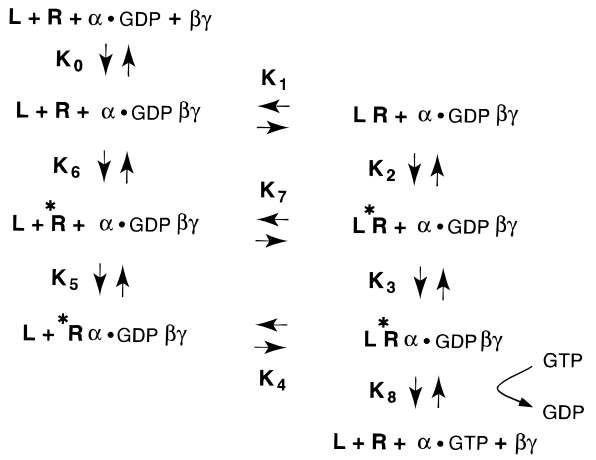

FIGURE 8: Scheme for the interactions of the receptor−G protein complex. L denotes ligand; R, the low affinity conformation of the receptor; *R, the high affinity conformation of the receptor; and *K*'s, equilibrium binding constants.

the receptor and the heterotrimer and the interaction between the agonist and the receptor−G protein complex.

Figure 8 presents a version of the extended ternary complex model proposed for the interaction of G proteins, seven transmembrane receptors, and ligands. This model accurately predicts the kinetic behavior of receptor systems and accounts for the constitutive activity of a number of mutant G protein coupled receptors (*51*). The scheme presented in Figure 8 is modified to highlight the important role of the $\beta\gamma$ dimer in the interaction of the heterotrimer with the receptor. The following observations presented in this report are consistent with the model: (a) the purified A_1 adenosine receptor exhibits two affinity states for agonists (Figures 3 and 4); (b) both α and $\beta\gamma$ subunits are required for receptor−G protein coupling (Figure 5 and (*1, 29*)); and (c) the purified receptors exhibit a low level of constitutive activity in the absence of ligand (Figure 5A).

In this study we examined the interactions diagramed in Figure 8 to determine how the composition of the $\beta\gamma$ dimer influences receptor−G protein coupling. Direct measurement of the equilibrium between the α subunit and the different $\beta\gamma$ dimers (K_D) in the absence of receptor shows that the affinity of the α subunit for $\beta_1\gamma_2$ and $\beta_1\gamma_1$ is similar (Figure 6 and Table 2). This finding is consistent with the crystal structures which show that the γ-subunit does not directly contact the α-subunit (*52,53*) and our experience in purifying the two dimers on an α-subunit affinity column. The $\beta_1\gamma_1$ and $\beta_1\gamma_2$ dimers appear to bind equally well and elute identically from the α column (*54*). Because the stability of the heterotrimer is not affected by the composition of the $\beta\gamma$ dimer, this equilibrium is not included in the other interactions shown in Figure 8.

Our analysis assumes that four other interactions are not affected by the composition of the $\beta\gamma$ dimer. The ability of the receptor itself to gain constitutive activity, *R (K_6) and the ability of ligand to bind to the basal, R, or constitutively active state of the receptor, *R, in the absence of heterotrimer (K_1, K_2, and K_7) are independent of the identity of the $\beta\gamma$ dimer. Thus, the steps identified by K_3, K_4, and/or K_5, involving the affinity the receptor for the G protein heterotrimer and the affinity of the agonist for the receptor−G protein complex are most likely to be affected by the composition of the $\beta\gamma$ dimer. This L*R$\alpha\beta\gamma$ complex represents the high affinity agonist binding conformation of the receptor (Figures 3 and 4) and is the entity which stimulates GTP/GDP exchange on the α subunit (Figure 5). An important finding is that the poor ability of the $\beta_1\gamma_1$ subunit to induce this conformation of the receptor cannot be overcome by increasing the amount of the $\beta\gamma$ dimer in the system (Figures 4B and 5B). Analogous results were obtained when a wide range of G protein heterotrimer concentrations was reconstituted into Sf9 cell membranes overexpressing the A_1 adenosine receptor (*1, 29*). These observations suggest that the affinity of the heterotrimer for the unliganded receptor (K_5) is not the major site affected by the different $\beta\gamma$ subunits. Thus, the decrement in high affinity binding and guanine nucleotide exchange activity observed using the $\beta_1\gamma_1$ dimer (Figures 4, 5, and 7) is most likely due to a difference in the L*R$\alpha\beta\gamma$ complex formed via the steps indicated in K_3 and/or K_4.

How can a difference in $\beta\gamma$ composition of the receptor−G protein complex modify ligand binding and agonist-stimulated GTP/GDP exchange? Two possibilities are that the *R$\alpha\beta\gamma$ containing $\beta_1\gamma_1$ has a lower affinity for ligand than the complex containing $\beta_1\gamma_2$ (a change in K_4) or that there is less *R$\alpha\beta\gamma$ formed in the presence of $\beta_1\gamma_1$ (a change in K_3). The data in Figure 7 indicates that the affinity of *R$\alpha\beta\gamma$ for ligand is less in the presence of $\beta_1\gamma_1$ since the off rate for ^{125}I-ABA is faster than in the presence of $\beta_1\gamma_3$. However, since the assay used in these experiments (high-affinity agonist binding) measures the formation of a L-*R-α-$\beta\gamma$ quaternary complex, the more rapid dissociation of ^{125}I-ABA from the complex containing a $\beta_1\gamma_1$ dimer may be due to instability of the association between L*R and $\alpha\beta\gamma$ (K_3). Our data does not distinguish between these two possibilities. An experimental probe (fluorescent label or crosslinking reagent) sensitive to changes in receptor conformation and allowing measurement of the *R state of the receptor independent of ligand binding would be useful for discriminating between these possibilities (*31, 55−57*). A complete understanding of this issue is important for understanding how the specificity of receptor−G protein interaction is achieved.

In is instructive to consider how the nature of the γ subunit affects the activity of the $\beta\gamma$ dimer in the extensively characterized visual signaling system (*30, 33, 34*). Kisselev and Gautam (*30*) investigated the ability of light-activated rhodopsin to stimulate the binding of GTPγS to the $G_t\alpha$ subunit in the presence of certain recombinant $\beta\gamma$ dimers and observed that the $\beta_1\gamma_1$ dimer was far more effective in supporting coupling than were $\beta_1\gamma_2$ or $\beta_1\gamma_3$ (*30*). Synthetic peptides derived from the C terminus of the γ subunit and chemically modified with geranyl, farnesyl, or geranylgeranyl groups were tested for their ability to stabilize meta-rhodopsin (*34*). The farnesylated peptide was much more potent in this assay than either the geranyl or geranyl-geranylated peptides, implying a specific interaction between the C terminus of the γ subunit and the receptor. These investigators also examined the affinity of the different $\beta\gamma$ dimers for the $G_t\alpha$ subunit using a precipitating antibody. They observed that all $\beta\gamma$ dimers were immunoprecipitated equally well with the α_t subunit. These results argue that the equilibrium between the $G_t\alpha$ subunit and the $\beta\gamma$ dimers tested is not affected by the nature of the $\beta\gamma$ subunit (results analogous to those shown in Figure 6 and Table 2). However, it appears that the composition of the γ subunit

in the $\beta\gamma$ dimer does have a marked effect on the ability of rhodopsin to couple to the $G_t\alpha$ subunit. Moreover, experiments performed using antisense mRNA to knock out certain G protein α and $\beta\gamma$ subunits capable of coupling to distinct receptors also suggest that different $\alpha\beta\gamma$ heterotrimers selectively couple to certain receptors (*15*−*20*). Overall, the data in this report combined with those obtained using antisense mRNA and the visual system argue that the composition of the $\beta\gamma$ dimer in the heterotrimer is an important determinant of receptor−G protein coupling.

In the current study, the observed differences in the ability of the $\beta_1\gamma_1$ and $\beta_1\gamma_2$ dimers to support receptor coupling must reside in the γ subunit as all other components in the assays are identical. Which domains in the γ subunit contribute to the observed specificity? Multiple lines of evidence suggest that the C-terminal amino acids and the type of prenyl group are critical determinants of γ interaction with receptors (*29, 33, 34*). Since there are large differences in amino acid sequence in the C terminus of γ_1 and γ_2 (48% identical or 61% similar over the final 21 amino acids) and differences in the prenyl groups (farnesyl in γ_1 as compared to geranylgeranyl in γ_2 or γ_3), these data argue that the receptor may have domains that can discriminate between both the peptide sequence and the prenyl groups (*8, 58*). The observation that the A_1 adenosine receptor does not couple well to a heterotrimer containing $G_{\alpha i2}$ and $\beta_1\gamma_1$ is not surprising in that rhodopsin, $G\alpha_t$, and $\beta_1\gamma_1$ are components of a structurally and functionally restricted signaling axis *in vivo*. However, another farnesylated γ subunit, γ_{11}, has been discovered by Ray et al. (*59*). This widely distributed γ-subunit is quite similar to γ_1 at the amino acid level (77% identical overall and 96% identical in the 21 C-terminal amino acids). Considering the emerging evidence that receptors recognize the C-terminal amino acids in the γ-subunit and the C-terminal lipid modification (*29, 30, 34*), there may be receptors that specifically interact with the γ_{11} subunit. It will be very interesting to determine the identity of these receptors and α subunits.

As noted above, the ability of $\beta\gamma$ dimers to activate certain effectors also depends on the nature of the γ subunit (*50, 60*−*62*). In most cases the maximal activity of different recombinant $\beta\gamma$ dimers has been similar, but the $\beta_1\gamma_1$ subunit is less potent than other dimers. This is the case for the ability of recombinant $\beta\gamma$ dimers to activate type II adenylyl cyclase (*50*), to stimulate phospholipase C-β_2 (*50*), to translocate βARK to the plasma membrane (*60, 61*), and to activate the muscarinic K^+ channel (*62*). The results obtained in the present study, using formation of the A_1*R-$\alpha\beta\gamma$ complex as the discriminator, are markedly different. In these assays, the $\beta_1\gamma_1$ dimer has proven to have approximately equal potency with $\beta_1\gamma_2$, but does not appear to be as effective (Figures 4B and 5B). The difference between $\beta\gamma$ interacting with effectors and receptors may be due to the fact that $\beta\gamma$ subunits interact with both the receptor and the α subunit, perhaps posing an additional constraint on the system.

In summary, the data in this report demonstrate that the specificity of receptor−G-protein interactions is affected by the nature of the γ-subunit in the heterotrimer. As the experiments were performed with four pure, recombinant proteins reconstituted into lipid vesicles, the data argue that protein−protein interactions alone have an impact on the specificity of A_1 adenosine receptor−G protein coupling. The results complement a growing body of literature demonstrating that the γ subunit is an important determinant of the specificity of receptor−G protein and G protein-effector coupling. As there are over 300 G protein coupled receptors (*5*) and at least 11 γ subunits (*59*), the possibilities for regulating the interactions between these molecules are numerous.

ACKNOWLEDGMENT

We thank Dr. Narasimhan Gautam for baculovirus encoding the γ_1 subunit, Dr. Rodney Biltonen for helpful discussion, and Dr. James LaDine of Affinity Sensors for advice on and protocols for immobilization of proteins on carboxymethyldextran.

REFERENCES

1. Figler, R. A., Graber, S. G., Lindorfer, M. A., Yasuda, H., Linden, J., and Garrison, J. C. (1996) *Mol. Pharmacol. 50*, 1587−1595.
2. Boyer, J. L., Graber, S. G., Waldo, G. L., Harden, T. K., and Garrison, J. C. (1994) *J. Biol. Chem. 269*, 2814−2819.
3. Lindorfer, M. A., Sherman, N. E., Woodfork, K. A., Fletcher, J. E., Hunt, D. F., and Garrison, J. C. (1996) *J. Biol. Chem. 271*, 18582−18587.
4. Simon, M. I., Strathmann, M. P., and Gautam, N. (1991) *Science 252*, 802−808.
5. Strader, C. D., Fong, T. M., Graziano, M. P., and Tota, M. R. (1995) *FASEB J. 9*, 745−754.
6. Neer, E. J. (1995) *Cell 80*, 249−257.
7. Gudermann, T., Kalkbrenner, F., and Schultz, G. (1996) *Ann. Rev. Pharmacol. Toxicol. 36*, 429−459.
8. Bourne, H. R. (1997) *Curr. Opin. Cell Biol. 9*, 134−142.
9. Wess, J. (1997) *FASEB J. 11*, 346−354.
10. Law, S. F., Manning, D., and Reisine, T. (1991) *J. Biol. Chem. 266*, 17885−17897.
11. Luthin, D. R., Eppler, C. M., and Linden, J. (1993) *J. Biol. Chem. 268*, 5990−5996.
12. McFadzean, I., Mullaney, I., Brown, D. A., and Milligan, G. (1989) *Neuron 3*, 177−182.
13. Spiegel, A. M., Simonds, W. F., Jones, T. L., Goldsmith, P. K., and Unson, C. G. (1990) *Biochem. Soc. Symp. 56*, 61−69.
14. Aragay, A. M., Katz, A., and Simon, M. I. (1992) *J. Biol. Chem. 267*, 24983−24988.
15. Kleuss, C., Hescheler, J., Ewel, C., Rosenthal, W., Schultz, G., and Wittig, B. (1991) *Nature 353*, 43−48.
16. Kleuss, C., Scherubl, H., Hescheler, J., Schultz, G., and Wittig, B. (1992) *Nature 358*, 424−426.
17. Kleuss, C., Scherubl, H., Hescheler, J., Schultz, G., and Wittig, B. (1993) *Science 259*, 832−834.
18. Kalkbrenner, F., Degtiar, V. E., Schenker, M., Brendel, S., Zobel, A., Heschler, J., Wittig, B., and Schultz, G. (1995) *EMBO J. 14*, 4728−4737.
19. Dippel, E., Kalkbrenner, F., Wittig, B., and Schultz, G. (1996) *Proceedings of the National Academy of Sciences of the United States of America 93*, 1391−1396.
20. Degtiar, V. E., Wittig, B., Schultz, G., and Kalkbrenner, F. (1996) *FEBS Lett. 380*, 137−141.
21. Butkerait, P., Zheng, Y., Hallak, H., Graham, T. E., Miller, H. A., Burris, K. D., Molinoff, P. B., and Manning, D. R. (1995) *J. Biol. Chem. 270*, 18691−9:
22. Chabre, O., Conklin, B. R., Brandon, S., Bourne, H. R., and Limbird, L. E. (1994) *J. Biol. Chem. 269*, 5730−5734.
23. Brandt, D. R., Asano, T., Pedersen, S. E., and Ross, E. M. (1983) *Biochemistry 22*, 4357−4362.
24. Brandt, D. R. and Ross, E. M. (1986) *J. Biol. Chem. 261*, 1656−1664.
25. Parker, E. M., Kameyama, K., Higashijima, T., and Ross, E. M. (1991) *J. Biol. Chem. 266*, 519−527.
26. Senogles, S. E., Spiegel, A. M., Padrell, E., Iyengar, R., and Caron, M. G. (1990) *J. Biol. Chem. 265*, 4507−4514.

27. Munshi, R. and Linden, J. (1990) *Mol. Pharmacol. 38,* 170−176.
28. Jockers, R., Linder, M. E., Hohenegger, M., Nanoff, C., Bertin, B., Strosberg, A. D., Marullo, S., and Freissmuth, M. (1994) *J. Biol. Chem. 269,* 32077−32084.
29. Yasuda, H., Lindorfer, M. A., Woodfork, K. A., Fletcher, J. E., and Garrison, J. C. (1996) *J. Biol. Chem. 271,* 18588−18595.
30. Kisselev, O. and Gautam, N. (1993) *J. Biol. Chem. 268,* 24519−24522.
31. Phillips, W. J. and Cerione, R. A. (1992) *J. Biol. Chem. 267,* 17032−17039.
32. Phillips, W. J., Wong, S. C., and Cerione, R. A. (1992) *J. Biol. Chem. 267,* 17040−17046.
33. Kisselev, O. G., Ermolaeva, M. V., and Gautam, N. (1994) *J. Biol. Chem. 269,* 21399−21402.
34. Kisselev, O., Ermolaeva, M., and Gautam, N. (1995) *J. Biol. Chem. 270,* 25356−25358.
35. Mulheron, J. G., Casanas, S. J., Arthur, J. M., Garnovskaya, M. N., Gettys, T. W., and Raymond, J. R. (1994) *J. Biol. Chem. 269,* 12954−12962.
36. Kozasa, T. and Gilman, A. G. (1995) *J. Biol. Chem. 270,* 1734−1741.
37. Patel, A., Craig, R. H., Daluge, S. M., and Linden, J. (1988) *Mol. Pharmacol. 33,* 585−591.
38. Nakata, H. (1989) *J. Biol. Chem. 264,* 16545−16551.
39. Graber, S. G., Figler, R. A., and Garrison, J. C. (1992) *J. Biol. Chem. 267,* 1271−1278.
40. Graber, S. G., Figler, R. A., Kalman-Maltese, V. K., Robishaw, J. D., and Garrison, J. C. (1992) *J. Biol. Chem. 267,* 13123−13126.
41. Laemmli, U. K. (1970) *Nature 227,* 680−685.
42. Liang, M. N. and Garrison, J. C. (1991) *J. Biol. Chem. 266,* 13342−13349.
43. Kohnken, R. E. and Hildebrandt, J. D. (1989) *J. Biol. Chem. 264,* 20688−20696.
44. Marquardt, D. M. (1963) *J. Soc. Indust. Appl. Math. 11,* 431−441.
45. Motulsky, H. J. and Ransnas, L. A. (1987) *FASEB J. 1,* 365−374.
46. Davies, R. J., Edwards, P. R., Watts, H. J., Lowe, C. R., Buckle, P. E., Yeung, D., Kinning, T. M., and Pollard-Knight, D. V. (1994) in *Techniques in Protein Chemistry V* (Crabb, J. W., Ed.) pp 285−292, Academic Press, New York.
47. Schuck, P. and Minton, A. P. (1996) *Trends Biochem. Sci. 21,* 458−460.
48. Heithier, H., Frolich, M., Dees, C., Baumann, M., Haring, M., Gierschik, P., Schlitz, E., Vaz, W. L. C., Hekman, M., and Helmreich, E. J. M. (1992) *Eur. J. Biochem. 204,* 1169−1181.
49. Neubig, R. R., Connolly, M. P., and Remmers, A. E. (1994) *FEBS Lett. 355,* 251−253.
50. Ueda, N., Iniguez-Lluhi, J. A., Lee, E., Smrcka, A. V., Robishaw, J. D., and Gilman, A. G. (1994) *J. Biol. Chem. 269,* 4388−4395.
51. Samama, P., Cotecchia, S., Costa, T., and Lefkowitz, R. J. (1993) *J. Biol. Chem. 268,* 4625−4636.
52. Wall, M. A., Coleman, D. E., Lee, E., Iniguez-Lluhi, J. A., Posner, B. A., Gilman, A. G., and Sprang, S. R. (1995) *Cell 83,* 1047−1058.
53. Lambright, D. G., Sondek, J., Bohm, A., Skiba, N. P., Hamm, H. E., and Sigler, P. B. (1996) *Nature 379,* 311−319.
54. Graber, S. G., Lindorfer, M. A., and Garrison, J. C. (1996) *Methods Neurosci. 29,* 207−226.
55. Taylor, J. M., Jacob-Mosier, G. G., Lawton, R. G., Remmers, A. E., and Neubig, R. R. (1994) *J. Biol. Chem. 269,* 27618−27624.
56. Gether, U., Lin, S., and Kobilka, B. K. (1995) *J. Biol. Chem. 270,* 28268−28275.
57. Taylor, J. M., Jacob-Mosier, G. G., Lawton, R. G., VanDort, M., and Neubig, R. R. (1996) *J. Biol. Chem. 271,* 3336−3339.
58. Wedegaertner, P. B., Wilson, P. T., and Bourne, H. R. (1995) *J. Biol. Chem. 270,* 503−506.
59. Ray, K., Kunsch, C., Bonner, L. M., and Robishaw, J. D. (1995) *J. Biol. Chem. 270,* 21765−21771.
60. Pitcher, J. A., Inglese, J., Higgins, J. B., Arriza, J. L., Casey, P. J., Kim, C., Benovic, J. L., Kwatra, M. M., Caron, M. G., and Lefkowitz, R. J. (1992) *Science 257,* 1264−1267.
61. Muller, S., Hekman, M., and Lohse, M. J. (1993) *Proc. Natl. Acad. Sci. U.S.A. 90,* 10439−10443.
62. Wickman, K. D., Iniguez-Lluhl, J. A., Davenport, P. A., Taussig, R., Krapivinsky, G. B., Linder, M. E., Gilman, A. G., and Clapham, D. E. (1994) *Nature 368,* 255−257.

BI972000Q